

Original Article

Reliability Analysis of Single Point Cutting Tool on Al6063 Alloy

K. Udayani¹, S. Gajanana², P. Laxminarayana³

^{1,3}Department of Mechanical Engineering, Osmania University, Hyderabad, India

²Department of Mechanical Engineering, MVSREC, Hyderabad, India

¹Corresponding Author : udhu28@gmail.com

Received: 09 August 2024

Revised: 11 September 2024

Accepted: 09 October 2024

Published: 30 October 2024

Abstract - This study aims to investigate the reliability of the Al6063 alloy machining of a single point cutting tool. Because of its well-known advantageous mechanical qualities, Al6063 can be used in a wide range of applications. The machining results are highly impacted by tool wear, such as flank wear, which makes prompt tool replacement necessary to preserve component quality and production efficiency. To assess tool performance, the experiment used High Speed Steel (HSS) tools under several cutting conditions, such as speed, feed, depth of cut, and rake angle. Using image processing methods, flank wear was assessed, and experimental data was used to simulate its distribution as a normal distribution. The probability that the cutting tool would function satisfactorily for the designated amount of time before needing to be replaced was ascertained using reliability analysis. The findings show that increased cutting forces improve tool reliability; in fact, some experiments had reliability percentages above 75%. The results highlight how crucial it is to maximize machining parameter optimization to extend tool life and reduce operational disturbances. To increase manufacturing productivity and quality assurance in Al6063 alloy applications, future research might concentrate on further optimizing these parameters and confirming the findings across various tool materials and machining environments.

Keywords - DOE, Flank wear, HSS tool, Process parameters, Reliability, Resultant Force.

1. Introduction

The combination of aluminum, silicon, and magnesium in Al 6063, a popular aluminum alloy, confers advantageous mechanical qualities, such as exceptional heat treatment and weldability. There is still a large study gap regarding the efficiency and reliability of single point cutting tools designed especially for Al 6063, even though many studies have examined the alloy's machinability and material characterization. The surface quality of machined components can be seriously compromised by tool wear processes such as crater development, built-up edges, and flank and nose wear. This can result in rework or tool replacement, which raises production costs. To maximize production efficiency and guarantee high-quality output, it is essential to comprehend the reliability of single point cutting tools while machining Al 6063. This study seeks to close this gap and eventually enhance manufacturing procedures and tool life management. Many life studies by J.G. Wager et al. [1] utilizing HSS tools for machining state that tool life values follow a statistical distribution that deviates from the normal distribution by about 0.3 of a coefficient of variation. The distribution patterns of normal and accelerated exams are similar, indicating a potential wider use for accelerated exams. It is important to remember that the commonly accepted concepts

of "constant" and "exponent" tool life are merely statistical mean values. Estimates of the probabilistic tool life are proposed, and the planned direction for further work is emphasized. The study by K Hitomi et al. [2] concentrated on the tool life's dependability analysis. Moreover, based on machining parameters and tool-wear limitations, it was shown that the reliability function may be utilized to compute the reliability swiftly. W.S. Lin [3] conducted multiple trials to evaluate the dependability variance of the cutting tool. Along with tool life and wear distribution, the trial data yields the dependability function and tool wear distribution. The reliability of the cutting tools at any given moment, the tool wear limit, and the cutting parameters for High-Speed Machining (HSM) may be easily ascertained with the help of the derived reliability function. A stochastic model is presented by El Wardany et al. [4] to forecast the tool failure rate while using ceramic tools to convert hardened steel. This model is predicated on the idea that the primary causes of the tool life ending are chemical wear, progressive wear, and early failure (such as chipping and breaking). Each reason for "tool failure" is believed to have a statistical distribution. General equations then represent the failure rate, reliability function, and tool-life distribution. Next, an experimental verification



of the assumed distributions is made. The coefficients of these equations are found using the experimental data. Researchers Konstantinos Salonitis et al. [5] looked at how the overall manufacturing efficiency is affected by the dependability of cutting tools. It is challenging to determine a cutting tool's exact remaining life as, in most circumstances, it can be utilized for several operations with various processing conditions. Based on sophisticated approximation techniques, the current study suggests a novel approach to cutting tool dependability estimates.

A widely used technique for structural reliability issues is reliability-based design/operation, which evaluates essential infrastructure performance under stochastic design parameters. The life of the cutting tools used in the machining processes has a significant impact on the components' quality. Chipping from tool damage may lead to the component being machined being trashed. As Carmen Elena Patino Rodriguez et al. [6] showed, it was expected that a normal distribution might be utilized to represent the tool's life. Finding the machining technique's operations sequence will allow you to determine how long each tool will run during the procedure. S. Ajmal Hussain et al. conducted an experimental analysis and comparison between silicon carbide and aluminum (6063) [7]. Aluminum and its parts are a great alternative to steel because of their low weight and resistance to corrosion, making them useful in both commercial and domestic contexts.

Steel is a well-known commodity that is used extensively in industries, and its price is always rising, which has an impact on manufacturing costs for both the home and automotive sectors. Because of this, it is imperative to swap out steel with a material that maintains the right weight ratio while being extremely robust and lightweight.

Al6063 is therefore utilized in this situation due to its strong tensile properties, good toughness, medium strength, moderate ductility, and resistance to corrosion. Siva Bhaskar et al.'s [8] approach for calculating the optimal time for the replacement of a tool is based on the tool performance determined by the dependability function. Oussama Zerti et al. [9] provided a method for determining the optimal machining parameters that yield a minimum of 23 surface roughness using the Taguchi approach.

Researchers Montasser S. Tahat et al. investigated the mechanical characteristics of the heat-treated 6063 aluminum alloy [10]. Aluminum alloy is appropriate for a variety of industrial applications due to its structural integrity. In addition to summarizing current patents, the study focused on the mechanical properties of the alloy in question following age hardening treatment. Abdalla Hassan Mihdy Jassim et al. [11] investigated the effects of heat treatments on aluminum alloy 6063's tensile behavior and toughness. After two hours of homogenization at 560°C, the alloy samples underwent a

one-hour solution heat treatment at 500, 530, and 560°C, and then they were quickly quenched in room-temperature water. The yield stress and tensile strength maximum values are 288.6 and 264.5 MPa, respectively. U. Lakshminarayana et al. used the dependability function to calculate a tool's performance to identify when it should be replaced. The study by Nithin M. Mali et al. includes shorter cycle times, adaptable procedures, compatible surface roughness, higher rates of material removal, and fewer environmental issues because cutting fluid is not required. However, it significantly increased tool wear and changed the quality and performance of the product due to the increased mechanical stress and heat generation.

Additionally, a CNC machine for dry machining was utilized, and an examination and comparison of the performance of uncoated and multilayer coated ($\text{Al}_2\text{O}_3+\text{TiC}+\text{TiNAlCrN}$) ceramic tools were carried out. A model for estimating tool wear and an experimental study on cutting tool wear was published by Vishal S. Sharma et al. [12]. We recode and analyze the variations in cutting force, vibration, and acoustic emission values with cutting tool wear. Adaptive Neuro Fuzzy Inference System (ANFIS) is used to construct a model for tool wear estimation in turning operations based on experimental data. The model has been developed using acoustic emission, vibrations and cutting forces in conjunction with time. This model estimates the cutting tool's wear rate. The model's wear estimation findings are compared with the actual outcomes and displayed. When comparing, the model produced results that were quite excellent. The addition of WC and group IV carbides to Ti(C, N) –was examined by Kwon et al. in [13]. Ni Cermet alters the microstructure, which modifies the material's properties. The mechanical characteristics and microstructure of AA6063 alloy reinforced with Palm Kernel Shell (PKS) powder were investigated by F.O. Edoziuno et al. [14]. Using the stir compo casting method, Al6063 matrix composites reinforced with different weight fractions of palm kernel shell particles (ranging from 2.5% to 15% at 2.5 intervals) were created. The mechanical characteristics and microstructure of the composites that were produced were examined and contrasted with those of the matrix alloy. The experimental findings demonstrated that the mechanical characteristics of the composites were enhanced.

2. Experimentation

2.1. Work Material Preparation

This involves the preparation of the cylindrical rod of Al6063 alloy material from casting, followed by machining for experimentation on the Lathe machine. The workpiece measures 240 mm in length and 25.4 mm in diameter. Table 5 has been developed from the experimental investigation. The various equipment used in performing the tests are a Lathe Machine, Work material, Tool materials, and Lathe Tool Dynamometer.

2.2. Optimum Composition of Al6063

Al6063 material of the following composition was used based on strength criteria, and the same material is used for this experimentation. This is the optimum composition of Al6063 alloy, having the highest tensile strength. All the machining parameters considered and the levels of each parameter are represented in Table 2, along with the units considered

2.3. Selection of Tool Material

The tool material used is an High-Speed Steel (HSS) tool for machining.

2.4. Design of Experiments (DOE)

To solve the problem with the necessary precision, as in Table 4, the DOE involves choosing the appropriate no. of trials and conditions under which to conduct them.

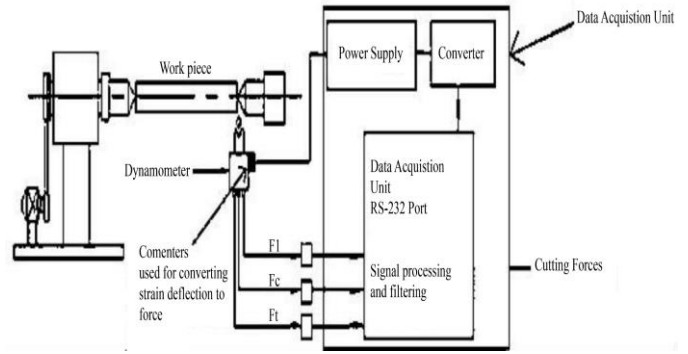


Fig. 3 Block diagram of experimental setup



Fig. 1 Casting of Al6063

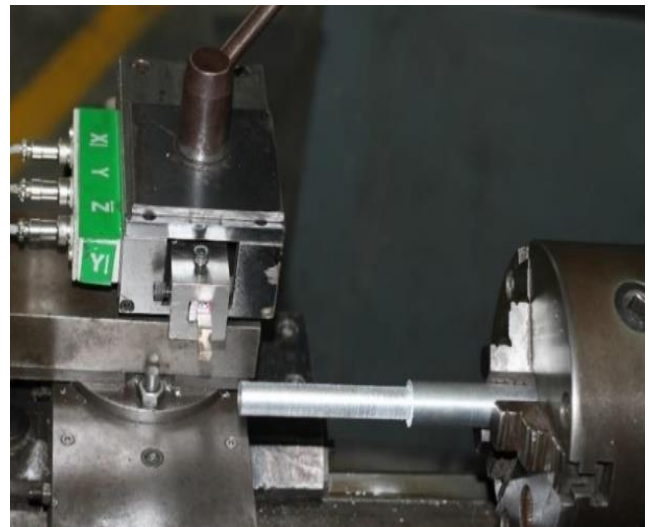


Fig. 4 Dynamometer setup with tool and job inserted



Fig. 2 Workpiece after machining

Table 1. The weight percentage of metals in Al6063

Metal	Mg	Si	Fe	Cu	Zn	Ti	Mn	Cr	Al
Wt %	0.45	0.2	0.3	0.1	0.1	0.05	0.05	0.1	98.65

Table 2. Input parameters with test levels

Factors	Units	Designation		Test levels	
		Actual form	Codedform	Low	High
Cutting speed	rpm	v	X1	150	445
Feed	mm/rev	f	X2	0.21	0.421
Depth of cut	mm	d	X3	0.2	0.5
Rake angle	degrees (°)	r	X4	15	20

Table 3. Chemical composition of Miranda HSS ZEDD tool

Tool Grade	Material Grade	Approximate % of metals					
		C	Cr	Mo	W	Co	V
ZEDD	M2	0.9	4.1	5.0	6.4	-	1.8

Table 4. Design matrix

Trial N ^o	v (rpm)	f (mm/rev)	d (mm)	r (°)
1	150	0.21	0.2	15
2	445	0.21	0.2	15

3	150	0.421	0.2	15
4	445	0.421	0.2	15
5	150	0.21	0.5	15
6	445	0.21	0.5	15
7	150	0.421	0.5	15
8	445	0.421	0.5	15
9	150	0.21	0.2	20
10	445	0.21	0.2	20
11	150	0.421	0.2	20
12	445	0.421	0.2	20
13	150	0.21	0.5	20
14	445	0.21	0.5	20
15	150	0.421	0.5	20
16	445	0.421	0.5	20

3. Observation of Flank Wear (VB)

For all 16 trials, flank wear is observed and is shown below in Figures 3 to 18

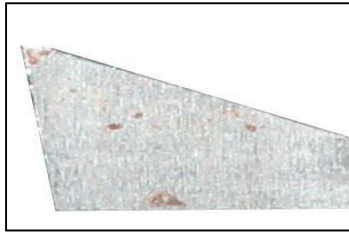


Fig. 5 Tool-1 geometry before and after experiment

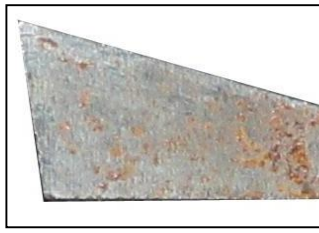


Fig. 6 Tool-2 geometry before and after experiment

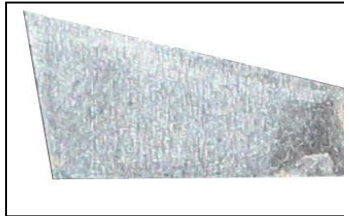


Fig. 7 Tool-3 geometry before and after experiment

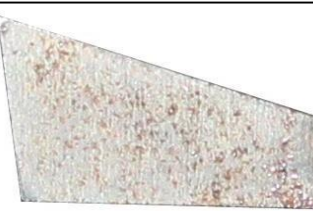


Fig. 8 Tool-4 geometry before and after experiment

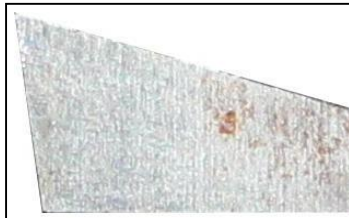


Fig. 9 Tool-5 geometry before and after experiment



Fig. 10 Tool-6 geometry before and after experiment

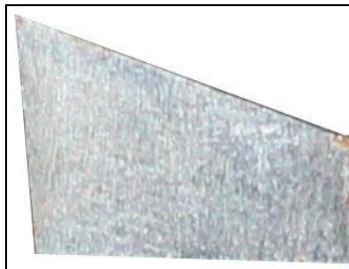


Fig. 11 Tool-7 geometry before and after the experiment

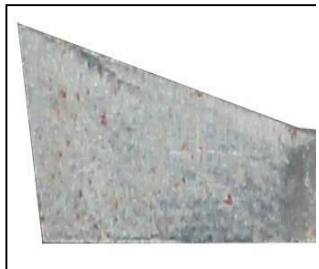
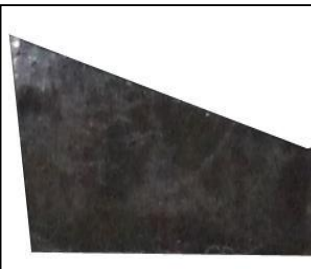


Fig. 12 Tool-8 geometry before and after the experiment



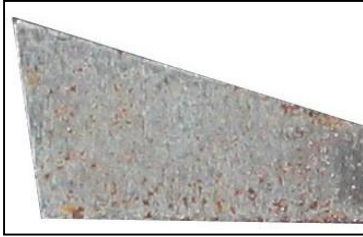


Fig. 13 Tool-9 geometry before and after experiment



Fig. 14 Tool-10 geometry before and after experiment



Fig. 15 Tool-11 geometry before and after experiment



Fig. 16 Tool-12 geometry before and after experiment



Fig. 17 Tool-13 geometry before and after experiment

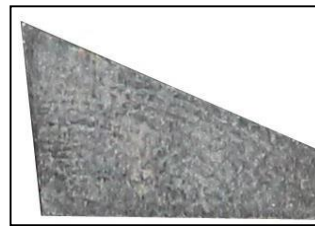


Fig. 18 Tool-14 geometry before and after experiment

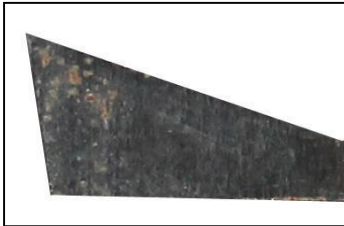


Fig. 19 Tool-15 geometry before and after experiment

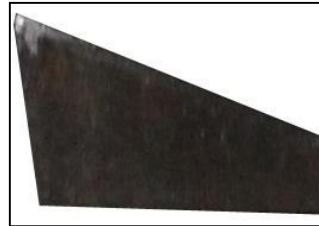


Fig. 20 Tool-16 geometry before and after experiment



3.1. Calculation of Flank Wear Using Image Processing

Flank wear detection using MATLAB code is mentioned in Figures 21 and 22.

```

Editor - C:\8 images new\tools\tool_moid.m
withhomo3.m  tool_moid.m  +
1  % Read in a standard MATLAB color demo image.
2  folder = 'C:\8 images new\tools final\16';
3  baseFileName = '2c.jpg';
4  % Get the full filename, with path prepended.
5  fullFileName = fullfile(folder, baseFileName);
6
7  rgbImage = imread(fullFileName);
8  grayImage = rgb2gray(rgbImage);
9  subplot(2, 2, 1);
10 imshow(grayImage);
11 title('Original Image', 'fontSize', fontSize);
12 % Enlarge figure to full screen.
13 set(gcf, 'Units', 'Normalized', 'OuterPosition', [0 0 1 1]);
14 % Logical Operation Approach.
15 thresholdValue = 200;
16 binaryImage = grayImage < thresholdValue; % Dark objects will be the chosen if you use <
17 % Do a "hole fill" to get rid of any background pixels inside the blobs.
18 binaryImage = imfill(binaryImage, 'holes');
19 % Display the binary image.
20 subplot(2, 2, 2);
21 imagesc(binaryImage);
22 colormap(gray(256));
23 title('Binary Image, obtained by thresholding', 'fontSize', fontSize);
24 % Label each object so we can make measurements of it
25 [labeledImage, numberOfRegions] = bwlabeln(binaryImage, 3);
26 subplot(2, 2, 3);
    
```

Fig. 21 Code in MATLAB

```

Editor - C:\8 images new\tools\tool_moid.m
withhomo3.m  tool_moid.m  +
21 imagesc(binaryImage);
22 colormap(gray(256));
23 title('Binary Image, obtained by thresholding', 'fontSize', fontSize);
24 % Label each object so we can make measurements of it
25 [labeledImage, numberOfRegions] = bwlabeln(binaryImage, 8);
26 subplot(2, 2, 3);
27 coloredLabels = label2rgb(labeledImage, 'hsv', 'k', 'shuffle'); % pseudo random color labels
28 imshow(coloredLabels);
29 title('Labeled Binary Image', 'fontSize', fontSize);
30
31
32 % Define object boundaries
33 boundaries = bwboundaries(binaryImage);
34 numberOfBoundaries = size(boundaries, 1);
35
36 for k = 1 : numberOfBoundaries
37     thisBoundary = boundaries(k);
38     boundaryx = thisBoundary(:, 2);
39     boundaryy = thisBoundary(:, 1);
40     plot(boundaryx, boundaryy, 'r-', 'LineWidth', 2);
41     num1 = string(boundaryx);
42     num2 = string(boundaryy);
43     a_col = append(num1);
44     b_col = append(num2);
45 end
46
    
```

Fig. 22 Code in MATLAB

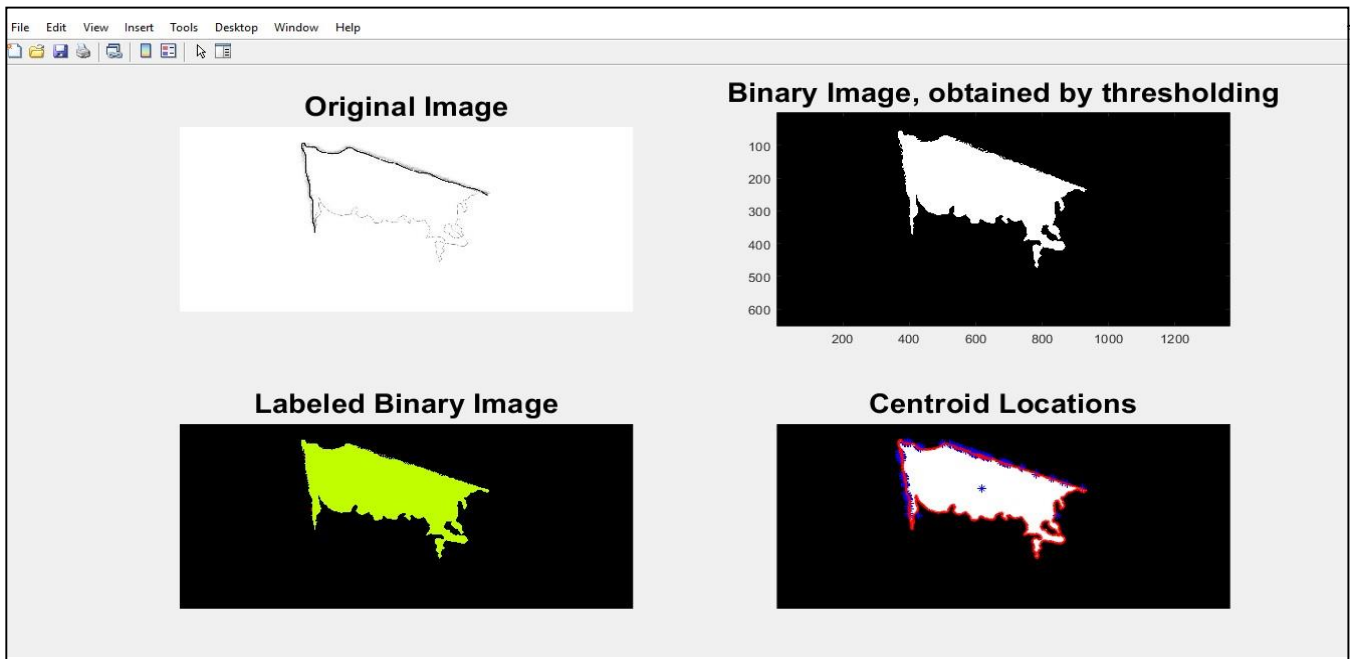


Fig. 23 Flank Wear detection in MATLAB

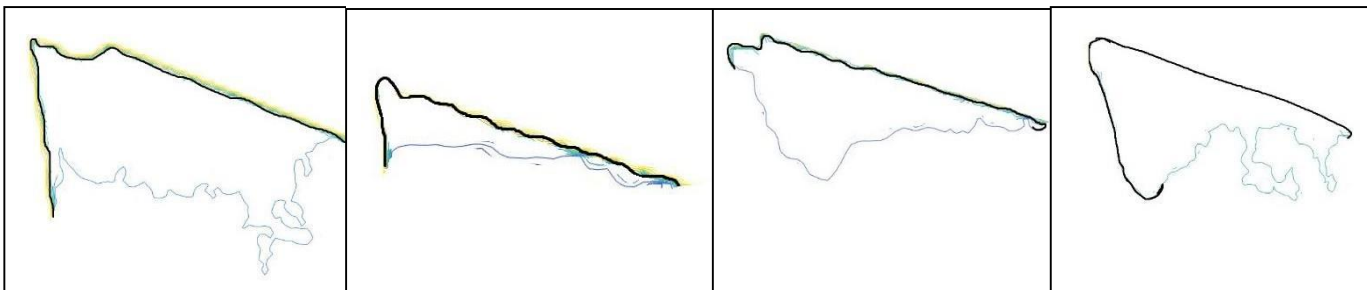
Flank wear detection of each trial specimen using image processing is shown below from trial 1 to trial 16, respectively.

VB = 0.1mm

VB= 0.07mm

VB = 1.45mm

VB = 0.36mm



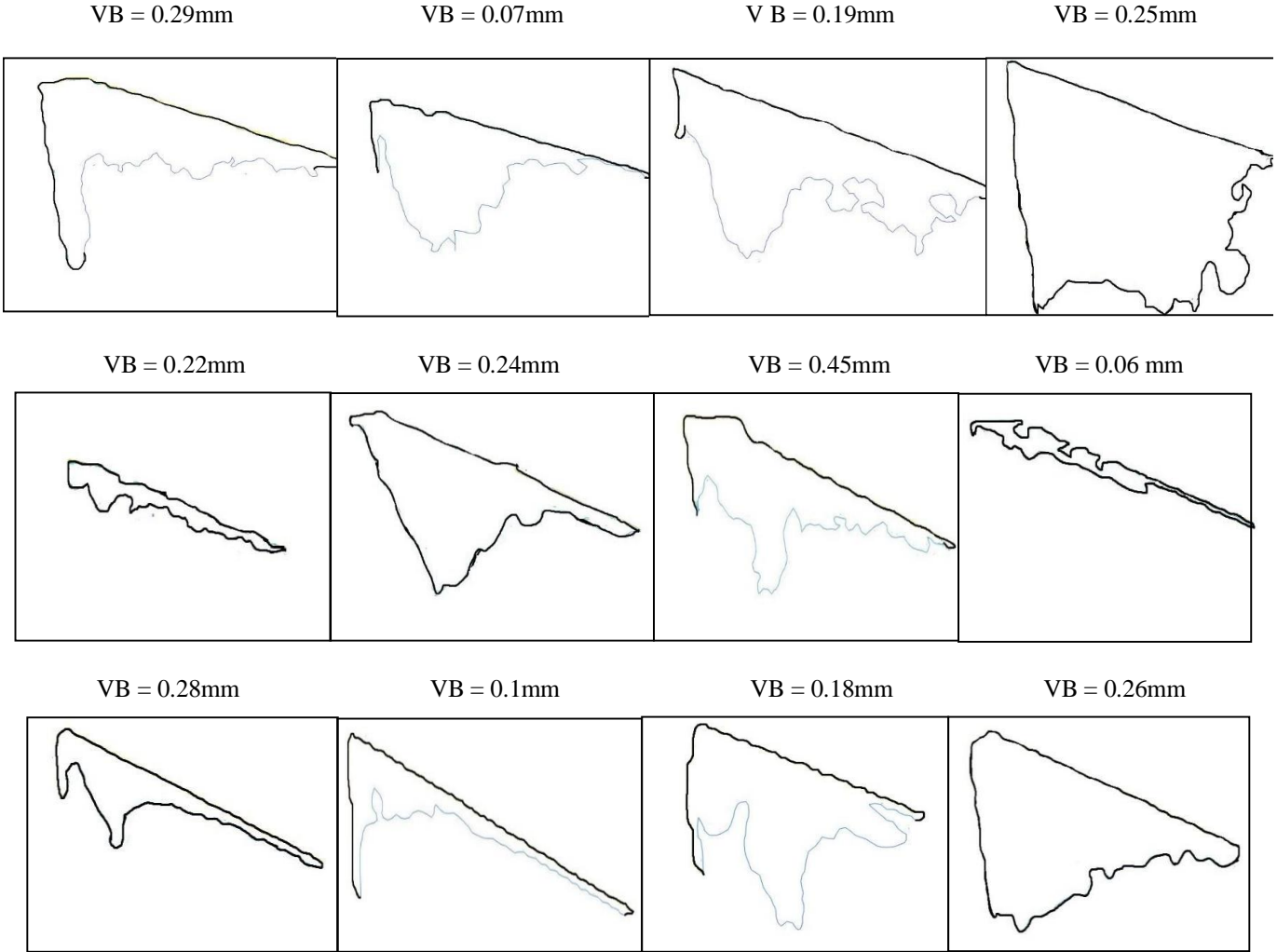


Fig. 24 Flank wear detection of each trial specimen using image processing

3.2. Calculation of Reliability

The tool life model assumes that flank wear follows a normal distribution. Drawing from Wager and Barash's [1971] extrapolation, Hitomi et al. [1979], and W.S. Lin [2008], the flank wear distribution's probability density function ($f(VB)$) can be expressed by the following formula:

$$f(VB) = \frac{1}{[\sqrt{2\pi}]\sigma} \exp\left(-\frac{(VB - \mu)^2}{2\sigma^2}\right) \quad (1)$$

If the function of (f), (d), (v) and (r) is the average VB, then,

$$\begin{aligned} VB &= \varnothing(v, f, d, r) \\ \mu &= E[VB] = E[\varnothing(v, f, d, r)] \\ \sigma &= \text{Var}[VB] = E[(VB - \mu)^2] \end{aligned}$$

There is an exponential relationship between VB and cutting parameters; thus, the flank wear is expressed by,

$$VB = C v^{b1} f^{b2} d^{b3} r^{b4}$$

Where C, b1, b2, b3 are constants which can be obtained

from experimentation. Now, the flank wear probability function is provided by,

$$f(VB) = \frac{1}{[\sqrt{2\pi}]\sigma} \exp\left(-\frac{(VB - C v^{b1} f^{b2} d^{b3} r^{b4})^2}{2\sigma^2}\right) \quad (2)$$

The likelihood of the turning tool being damaged occurred prior to time t:

$$P(\tau < t) = \left[\int_0^t f(\tau) d\tau \right] \quad (3)$$

The likelihood that flank wear will reach the life limit at time t is VB^* if the flank wear at tool life end is:

$$P(VB \geq VB^*) = 1 - \left[\int_0^{VB^*} f(VB) dVB \right] \quad (4)$$

Then,

$$\left[\int_0^t f(\tau) d\tau \right] = \left[\int_0^{VB^*} f(VB) dVB \right] \quad (5)$$

$$R(t) = 1 - \Phi \left[\frac{T_v - \mu}{\sigma} \right]$$

On substituting f(VB) into equation (5), rearranging and differentiating with respect to t, the probability density function of tool life f(t) is

$$f(t) = \frac{1}{\sqrt{2\pi}\sigma} \exp \left[- \left(\frac{T_v - t}{\sqrt{2}\sigma} \right)^2 \right]$$

When the average value of flank wear reaches VB*, the time Tv is reached. The following equation can be used to get the reliability function R(t).

$$R(t) = 1 - P(\tau < t)$$

$$= 1 - \int_{-\infty}^t \frac{1}{\sqrt{2\pi}\sigma} \exp \left[- \frac{1}{2} \left(\frac{x - \mu}{\sigma} \right)^2 \right] dx$$

However, there is no closed form of solution to this integral, so the transformation Z is given by,

$$Z = \frac{T_v - \mu}{\sigma}$$

As a result, the general cutting tool reliability equation based on the failure event is provided by,

Thus, R(t) = 1 - Φ(Z)

Where Φ(Z) is the probability of failure of the tool, Hence, R(t) = 1 - P(t)

The value of Z is chosen from the normal distribution table.

3.3. Metal Removal Rate (MRR)

The amount of material removed in millimetres per minute (mm³) during turning operations is known as the MRR. Each turning of the workpiece results in the removal of a ring-shaped layer of material.

$$MRR = \frac{W_b - W_a}{\rho * t} \frac{mm^3}{min}$$

Where, ρ is the material's density (gm/mm³), t is the machining time (min), W_b is the workpiece's weight before machining, and W_a is the workpiece's weight after machining (gm). Table 5 has been developed from the experimental investigation.

Table 5. Result table

Trial No.	v (rpm)	f (mm/rev)	d (mm)	r (°)	Machining Time t (min)	Flank Wear VB (mm)	Resultant Force (kgf)
1	150	0.21	0.2	15	3.11	0.1	22.95
2	445	0.21	0.2	15	1.05	0.07	71.48
3	150	0.421	0.2	15	1.55	1.45	99.08
4	445	0.421	0.2	15	0.53	0.36	70.93
5	150	0.21	0.5	15	3.1	0.29	8.60
6	445	0.21	0.5	15	1.05	0.07	14.56
7	150	0.421	0.5	15	1.54	0.19	34.67
8	445	0.421	0.5	15	0.52	0.25	43.60
9	150	0.21	0.2	20	3.08	0.22	70
10	445	0.21	0.2	20	1.04	0.24	47.09
11	150	0.421	0.2	20	1.56	0.45	23.17
12	445	0.421	0.2	20	0.52	0.06	6.72
13	150	0.21	0.5	20	1.02	0.28	11.88
14	445	0.21	0.5	20	1.04	0.1	13.07
15	150	0.421	0.5	20	1.54	0.18	17.03
16	445	0.421	0.5	20	0.52	0.26	15.76

Table 6. Calculation of reliability

Trial No.	Flank wear VB (mm)	t (min)	T _v	Z	Probability of failure (%)	Reliability (%)
1	0.1	3.11	1.86	4.95	-	-
2	0.07	1.05	0.9	1.93	97.32	2.68
3	1.45	1.54	0.06	-0.707	24.20	75.8
4	0.36	0.53	0.08	0.644	73.89	26.11
5	0.29	3.1	0.64	1.116	86.65	13.35
6	0.07	1.05	0.9	1.933	97.32	2.68
7	0.19	1.54	0.48	0.613	72.91	27.09

8	0.25	0.52	0.12	-0.518	30.5	69.5
9	0.22	3.08	0.04	-0.770	22.06	77.94
10	0.24	1.04	0.26	-0.078	47.21	52.79
11	0.45	1.56	0.20	-0.267	39.74	60.26
12	0.06	0.52	0.52	0.738	76.73	23.27
13	0.28	1.02	0.21	-0.235	40.9	59.1
14	0.1	1.04	0.62	1.053	85.31	14.69
15	0.18	1.54	0.51	0.707	75.8	24.2
16	0.26	0.52	0.12	-0.518	30.5	69.5

Mean of flank wear (μ) = 0.285, Standard deviation of flank wear (σ) = 0.3181

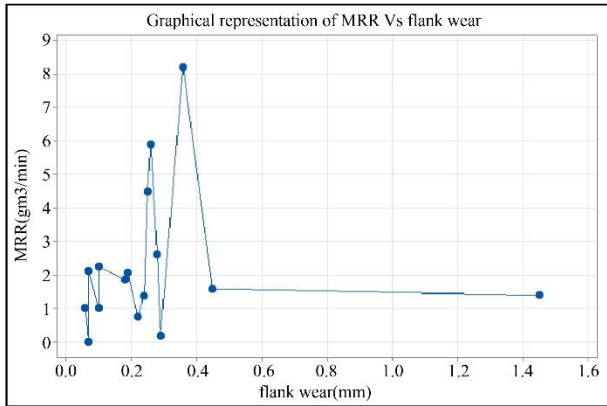


Fig. 25 MRR Vs flank wear

From the above graph, it is observed that the highest MRR is $8.19\text{gm}^3/\text{min}$, and the corresponding flank wear is 0.36mm for Figure 4, for which the machining parameters are $v = 445\text{rpm}$, $f = 0.421\text{mm}/\text{rev}$, $d = 0.2\text{mm}$ and $r = 15^\circ$. The lowest MRR is $0.02\text{gm}^3/\text{min}$, and the corresponding flank wear is 0.07mm for Figure 2, for which the machining parameters are $v = 445\text{rpm}$, $f = 0.21\text{mm}/\text{rev}$, $d = 0.2\text{mm}$ and $r = 15^\circ$.

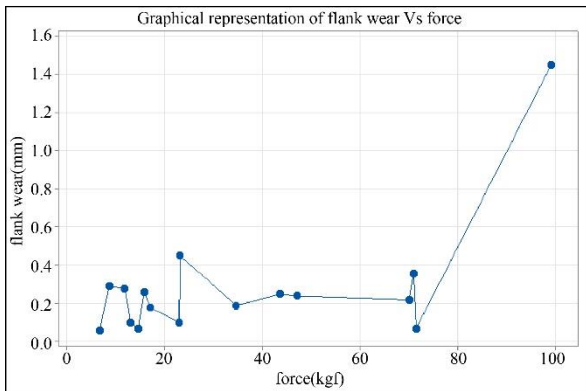


Fig. 26 flank wear Vs force

From the above graph, it is observed that the highest flank wear is 1.45mm , and the corresponding cutting force is 99.08kgf for Figure 3, for which the machining parameters are $v = 150\text{rpm}$, $f = 0.421\text{mm}/\text{rev}$, $d = 0.2\text{mm}$ and $r = 15^\circ$. The lowest flank wear is 0.06mm , and the corresponding cutting force is 6.72kgf for Figure 12, for which the machining

parameters are $v = 445\text{rpm}$, $f = 0.421\text{mm}/\text{rev}$, $d = 0.2\text{mm}$ and $r = 20^\circ$

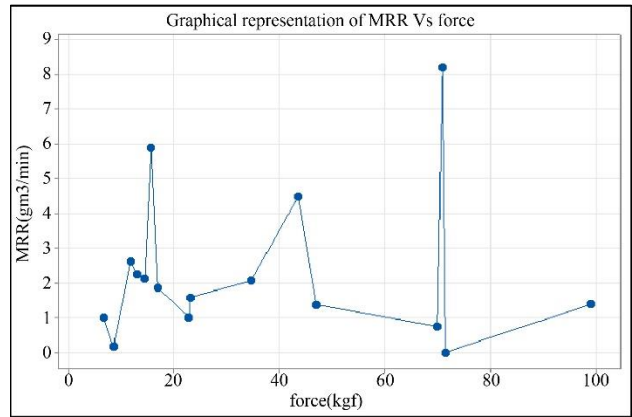


Fig. 27 MRR Vs force

From the above graph, it is observed that the highest MRR is $8.19\text{gm}^3/\text{min}$, and the corresponding cutting force is 70.93kgf for Figure 4, for which the machining parameters are $v = 445\text{rpm}$, $f = 0.421\text{mm}/\text{rev}$, $d = 0.2\text{mm}$ and $r = 15^\circ$. The lowest MRR is $0.02\text{gm}^3/\text{min}$, and the corresponding cutting force is 71.48kgf for Figure 2, for which the machining parameters are $v = 445\text{rpm}$, $f = 0.21\text{mm}/\text{rev}$, $d = 0.2\text{mm}$ and $r = 15^\circ$.

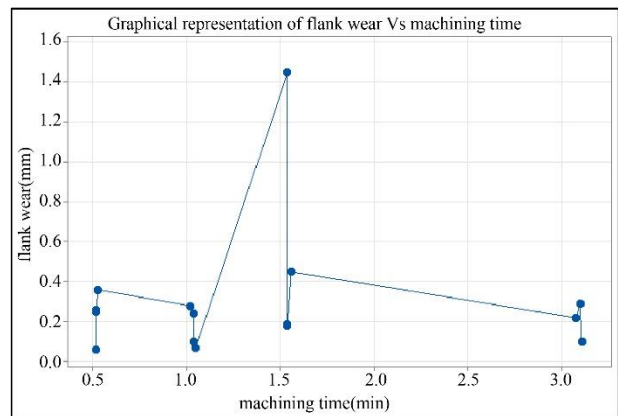


Fig. 28 flank wear Vs machining time

From the above graph, it is observed that the highest flank wear is 1.45mm, and the corresponding machining time is 1.54min for Figure 3, for which the machining parameters are $v = 150\text{rpm}$, $f = 0.421\text{mm/rev}$, $d = 0.2\text{mm}$ and $r = 15^\circ$. The lowest flank wear is 0.06mm, and the corresponding machining time is 0.52min for Figure 12, for which the machining parameters are $v = 445\text{rpm}$, $f = 0.421\text{mm/rev}$, $d = 0.2\text{mm}$ and $r = 20^\circ$.

There are significant implications for industrial productivity, cost savings, and product quality from the reliability analysis of single point cutting tools, especially when machining Al6063 alloy. In the sections that follow, we go over possible industrial applications and provide examples of how reliability analysis has been applied to improve production efficiency.

- **Optimized Tool Replacement Strategies**
By reducing unscheduled downtime, reliability analysis can help industries choose the best times to replace their tools. Businesses can use a just-in-time replacement strategy by forecasting the lifespan of cutting tools based on their wear patterns.
- **Case Study: Automotive Component Manufacturing**
In an automotive parts manufacturer, reliability analysis led to a 20% reduction in tool replacement costs. By shifting from reactive to predictive maintenance—based on the reliability functions derived from experimental wear data—the company reduced machining downtime and improved throughput.
- **Enhanced Process Parameter Selection**
Manufacturers can more effectively choose process variables (feed rate, rake angle, and cutting speed) that optimize tool life while preserving product quality by using reliability analysis. This modification enhances overall machining performance in addition to prolonging the life of cutting tools.
- **Example: Aerospace Industry**
An aircraft component manufacturer used reliability analysis to identify the ideal machining conditions for Al6063 components. They consequently increased production

efficiency by 30% and significantly decreased scrap rates, which are directly related to improved tool life and performance predictability. The results of the single point cutting tool reliability investigation on Al6063 alloy have wide-ranging effects on several industrial applications. Manufacturers can reap significant operational benefits by increasing production efficiency, cutting expenses, and maximizing tool life. To further improve manufacturing processes, future research could broaden these applications by investigating the incorporation of cutting-edge materials and technologies into the reliability framework.

4. Conclusion

According to the obtained data, for Fig-9, with machining inputs of $v = 150\text{ rpm}$, $f = 0.21\text{ mm/rev}$, $d = 0.2\text{ mm}$ at $r = 20^\circ$ and observed cutting force of 70 kgf, exhibited the maximum reliability of 77.94%. The force of 70 kgf corresponds to an MRR of $0.763\text{ cm}^3/\text{min}$. This concludes that high cutting force is required for the tool to be more reliable. The tool replacement time is suggested to be 3 minutes, which is indicated for minimum MRR.

Limitations of the Study

Due to the controlled laboratory setting in which the studies were carried out, actual industrial settings might not be perfectly replicated. Changes in temperature, humidity, and other environmental conditions may impact tool wear and reliability. Even though Al6063 alloy was utilized consistently, the machining results could be impacted by differences in the material's composition and microstructure between batches. Any variations in grain structure or impurity levels could result in uneven tool performance. Other tool materials, such as carbide and ceramic, were not evaluated; instead, the study concentrated on High-Speed Steel (HSS) tools. The findings may be limited by the fact that various materials may display distinct wear profiles under comparable machining settings. The findings may not fully translate to all industrial settings due to differences in production volumes, machining strategies, and economic constraints faced by manufacturers.

References

- [1] Abdalla H. Mihdy Jassim, "Effect of Heat Treatments on the Tensile Properties and Impact Toughness of 6063 Aluminium Alloy," *Al-Qadisiyah Journal of Pure Science*, 2015. [[Google Scholar](#)] [[Publisher Link](#)]
- [2] Bhaskar, A. Siva, and Venkata Ramesh Mamilla, "A Reliability Based Approach for Predicting Optimal Tool Replacement Time," *International Journal of Scientific Research in Knowledge*, 2013. [[Google Scholar](#)]
- [3] Carmen Elena Patiño Rodriguez, and Gilberto Francisco Martha de Souza, "Reliability Concepts Applied to Cutting Tool Change Time," *Reliability Engineering & System Safety*, vol. 95, no. 8, pp. 866-873, 2013. [[CrossRef](#)] [[Google Scholar](#)] [[Publisher Link](#)]
- [4] T. I. El Wardany, and M. A. Elbestawi, "Prediction of Tool Failure Rate in Turning Hardened Steels," *The International Journal of Advanced Manufacturing Technology*, vol. 13, pp. 1-16, 1997. [[CrossRef](#)] [[Google Scholar](#)] [[Publisher Link](#)]
- [5] J. G. Wager, and M. M. Barash, "Study of the Distribution of the Life of HSS Tools," *Journal of Manufacturing Science and Engineering*, vol. 93, no. 4, pp. 1044-1050, 1971. [[CrossRef](#)] [[Google Scholar](#)] [[Publisher Link](#)]
- [6] K. Hitomi, N. Nakamura, and S. Inoue, "Reliability Analysis of Cutting Tools," *Journal of Manufacturing Science and Engineering* vol.101, no. 2, pp. 185-190, 1979. [[CrossRef](#)] [[Google Scholar](#)] [[Publisher Link](#)]

- [7] Konstantinos Salonitis, and Athanasios Kolios, “Reliability Assessment of Cutting Tools Life Based on Advanced Approximation Methods,” *Procedia CIRP*, vol. 8, pp. 397-402, 2013. [[CrossRef](#)] [[Google Scholar](#)] [[Publisher Link](#)]
- [8] Won Tae Kwon, June Seuk Park, and Shinhoo Kang, “Effect of Group IV Elements on the Cutting Characteristics of Ti(C,N) Cermet Tools and Reliability Analysis,” *Journal of Materials Processing Technology*, vol. 166, no. 1, pp. 9-14, 2005. [[CrossRef](#)] [[Google Scholar](#)] [[Publisher Link](#)]
- [9] Montasser S. Tahat, Nadim A. Emira, and Hamzeh T. Mohamad, “Study of the Mechanical Properties of Heat Treated 6063 Aluminium Alloy”, *Recent Patents on Mechanical Engineering*, 2010. [[Google Scholar](#)] [[Publisher Link](#)]
- [10] Nithin M Mali, and T. Mahender, “Wear Analysis of Single Point Cutting Tool with And Without Coating,” *International Journal of Research in Engineering and Advanced Technology*, vol. 3, no. 3, pp. 49-57, 2015. [[Google Scholar](#)]
- [11] Oussama Zerti et al., “Taguchi Design of Experiments for Optimization and Modeling of Surface Roughness When Dry Turning X210Cr12 Steel”, *In Proceedings Applied Mechanics, Behavior of Materials, and Engineering Systems*, pp. 275-288, 2014. [[CrossRef](#)] [[Google Scholar](#)] [[Publisher Link](#)]
- [12] Vishal S. Sharma, S. K. Sharma, and Ajay K. Sharma, “Cutting Tool Wear Estimation for Turning,” vol. 19, pp. 99-108, 2007. [[CrossRef](#)] [[Google Scholar](#)] [[Publisher Link](#)]
- [13] W.S. Lin, “The Reliability Analysis of Cutting Tools in the HSM Processes”, *International Scientific Journal published monthly by the World Academy of Materials and Manufacturing Engineering*, vol. 30, no. 2 pp. 97-100, 2008. [[CrossRef](#)] [[Google Scholar](#)] [[Publisher Link](#)]
- [14] F.O. Edoziuno et al., “Mechanical And Microstructural Characteristics of Almuinium 6063 Alloy/Palm Kernell Shell Composites for Lightweight Applications” *Scientific African*, vol. 12, 2021. [[CrossRef](#)] [[Google Scholar](#)] [[Publisher Link](#)]